ELSEVIER

Catalysis Today 36 (1997) 485–496

CATALYSIS TODAY

New strategy of creation of local catalytic sites in definite electronic and coordination states

Alexei A. Slinkin*, Alexei V. Kucherov

N.D. Zelinsky Institute of Organic Chemistry, Russian Academy of Sciences, Leninsky Prosp. 47, B-334 Moscow, Russia

---

Abstract

Atomic-scale engineering of catalytic functions of isolated redox sites in confined environments of zeolitic channels is proposed as a new approach to the investigation of structure–properties relationship in heterogeneous 'biomimetic' catalysis. It is shown that the design of such catalysts, on the base of high-silica zeolites, containing isolated transition-metal cations as active redox sites, may present promising opportunities for creation of new types of contacts from a practical point of view. A detailed analysis of transition-metal cation incorporation into high-silica zeolites by either conventional or solid-state exchange is given. Stabilization of one or several transition-metal ions by matrices of high-silica zeolites (mainly H-ZSM-5) is discussed. The influence of different factors on the processes of cationic-species stabilization is analyzed. These data are correlated with the results of catalytic testing in reactions of total oxidation of hydrocarbons (HC), direct decomposition of NO_x, and SCR of NO_x by HC. The relationship between catalytic activity and selectivity of cationic sites and their coordination and electronic state, regulated by either thermal treatment or introduction of different anionic ligands, is analyzed.

Keywords: High-silica zeolite; Transition metal cation; Solid-state exchange

---

1. Introduction

The mechanism of activation of reactants on the surface of heterogeneous catalysts is determined by the nature of the active site. However, a very complex mixture of clustered and isolated ions, differing in both coordination and valence state, normally presents itself on the surface of supported heterogeneous catalysts. Therefore, it is usually impossible to differentiate between these sites for a correct correlation of intrinsic catalytic properties and physical properties of the isolated sites.

Synthesis of inorganic 'biomimetic' catalysts on the basis of high-silica zeolites, containing isolated transition-metal cations as active redox sites, opens the way for creation of new types of catalysts. The term 'biomimetic' is used to point out that the catalytic behavior of isolated transition-metal cations in a specific environment of zeolitic matrix could be similar to the action of active places of enzymes. Nanometer-scale engineering of catalytic functions of isolated redox sites in the confined environments of zeolitic channels is of great interest. This diluted system, with crystalline zeolitic matrix and some discrete sites of cation location, is quite simple for characterization by physical methods and permits a

---

*Corresponding author.

PII S0920-5861(96)00239-8

correct structure–properties correlation for 'isolated' catalytic sites.

The aim of the present work is to summarize our data on the nature and catalytic properties of an isolated redox site (transition-metal ion), stabilized in the zeolitic matrix (mainly ZSM-5).

2. Results and discussion

In our study, electron spin resonance (ESR) is used mainly for physical characterization of the samples. The intensities of the lines and the parameters of the spectra allow the determination of the cation concentration and the identification of the type of coordination for many transition-metal ions (Cu^{2+}, Mn^{2+}, Cr^{3+}, Fe^{3+}, V^{4+}, Cr^{5+} and Mo^{5+}). The in situ monitoring of their interaction with different molecules gives very important additional information for correlation with the data of catalytic testing.

The samples under investigation are tested in catalytic oxidation of alkanes (CH_4, C_2H_6), N_2O catalytic decomposition, and NO_x selective reduction.

A conventional ion exchange from solutions can be used for introduction of a few bicharged ions, but many transition-metal cations could be introduced by a solid-state reaction between H^- or NH_4^- forms of zeolites and different transition-metal compounds [1].

The simplified schemes illustrate the chemistry of the solid-state interaction between metal salts or oxides (e.g., copper) and isolated protonic sites in the H-form zeolite:

$$CuCl_2 + (H^+) - \text{zeolite} \rightarrow (CuCl^+) - \text{zeolite} + HCl$$

$$CuSO_4 + (H^+) - \text{zeolite} \rightarrow (CuHSO_4^+) - \text{zeolite}$$

$$CuO + (H^+) - \text{zeolite} \rightarrow (CuOH^+) - \text{zeolite}$$

where (H^+) is the strong Broensted acid site of zeolite (e.g., H-ZSM-5). The first reaction is in use for quantitative determination of the exchange degree by the titration of eliminated HCl (Karge et al.). The two other examples show the processes without elimination of the side products from the H-zeolite.

The samples prepared by both convenient ion exchange from solutions as well as solid-state ion-exchange methods were investigated.

3. Physical properties of transition-metal cations stabilized by H-ZSM-5 matrix

3.1. Copper ions

The introduction of copper in H-ZSM-5 samples of different SiO_2/Al_2O_3 ratio gives Cu(II) ESR signals which were identical in hyperfine structure (hfs), but differed in the signal intensities. A linear correlation between maximum intensity of Cu(II) ESR signal and Al^{3+} content in ZSM-5 framework was established [2], demonstrating clearly that the number of cationic vacancies for Cu(II) ions (protonic sites) is determined by the Al content in ZSM-5.

The Cu/H-ZSM-5 samples, calcined at 550°C, contain two types of isolated Cu^{2+} cations located in a square-planar environment ($g_{11}= 2.27$; $A_{11} = 175$ Oe) and a five-coordinated one ($g_{11} = 2.31$; $A_{11} = 155$ Oe)

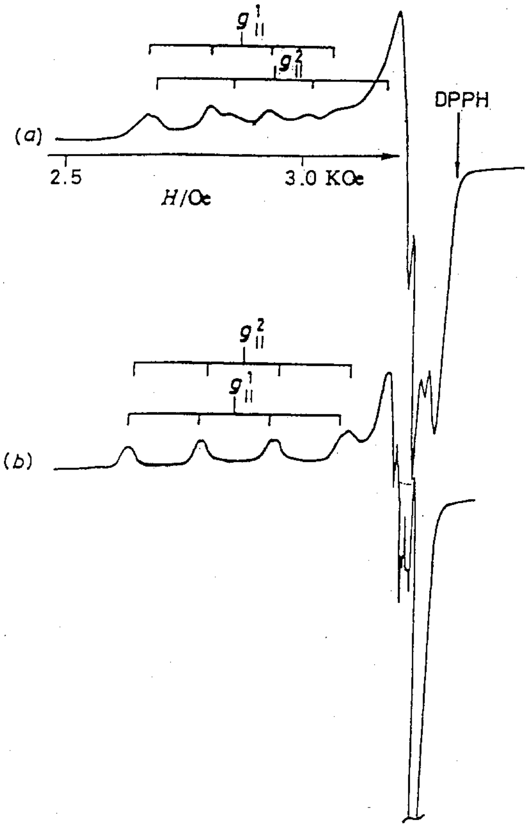

Fig. 1. ESR spectra at 20°C, for Cu-ZSM-5: (a) calcined at 550°C and evacuated and (b) calcined at 800°C and evacuated [2].

(Fig. 1). The spectra of the samples, calcined at 800°C, show the preservation of the two discrete types of Cu^{2+}-ion sites, but distorted with respect to the two previous ones. The strong influence of O_2 on the hfs of Cu(II) ESR spectra is also typical of the exchanged sample Cu/H-ZSM-5 [3]. It is concluded that the Cu(II) ions, which migrate into H-ZSM-5 from the outer surface of the crystals, are coordinated at the same positions as the isolated Cu^{2+} cations introduced by conventional ion exchange. Upon calcination, the number of isolated Cu^{2+} ions in H-ZSM-5 reaches a maximum of 30–40% of the Al^{3+} framework [2].

The acid sites in high-silica zeolites may be considered as powerful traps for Cu(II) ions which migrate into the zeolitic channels upon calcination. Formally, the process may be considered as the reaction of copper compounds with a strong acid (protonic sites in high-silica zeolites).

In H-ZSM-5, Cu(II) compensates one elemental charge of the lattice and has an additional link to an extra-lattice ligand ($(Cu(OH)^+)$) [3]. The study of the interaction of H-ZSM-5 with CuF_2, $CuCl_2$, $Cu_3(PO_4)_2$ [3], and $CuSO_4$ [4] demonstrated the influence of the anion (extra-lattice ligand). Differences in the types of Cu(II) coordination due to the presence of different anions were clearly seen [3,4], and it was concluded that a considerable part of the isolated Cu^{2+} cations in zeolite channels interact with extra-lattice ligands, such as F^- or $(PO_4)^{3-}$.

There is only one XRD work [5] on the location of Ni^{2+} in H-ZSM-5. Two sites were detected: the first site is near the wall of the straight elliptical channel, and the second one is inside the element, $T_{14}O_{20}$, composed entirely of five-membered rings. The cation in the main channel is linked with three lattice oxygens and must be coordinated with extra-lattice ligands. The second site with six lattice-oxygen ligands is recessed from the main channels of ZSM-5, and its geometry is presented in Fig. 2. In [6] it was assumed that Cu^{2+} cations are located in the same sites of ZSM-5 as Ni^{2+} cations, and the properties of such a location (Fig. 2) were analyzed by means of quantum-chemical calculations. It was shown that calculated components of the g-tensor agree well with the experimental ones. At the same time, quantum-chemical calculations showed that a small geometric displacement of the Cu^{2+} ion in its chelate site may result in a drastic change in the g-factor values. A noticeable change in g-components accompanied even a negligible Cu^{2+} ion displacement ($Z = 0.01$ A). The aforementioned INDO calculations confirmed the surprising effect of measurable changes in the hfs of the Cu^{2+} ESR signal upon the physisorption of Xe or n-hexane inside Cu/H-ZSM-5 channels [7].

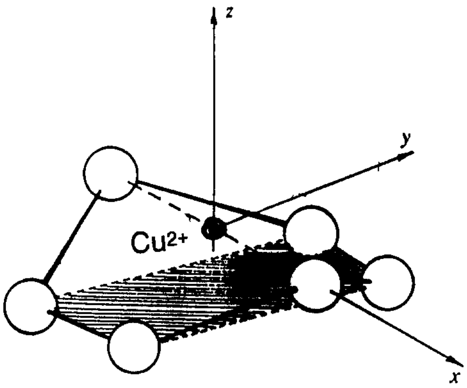

Fig. 2. Cluster model of an isolated Cu(II) ion inside a H-ZSM-5 structural fragment composed of five-membered rings (taken from X-ray data [5,6]).

Interaction of different molecules with Cu(II) ions in Cu-ZSM-5 was studied in [6,8–10]. It was shown that factors other than the possibility of coordinative complex formation in zeolitic channels must also be taken into account when analyzing the mechanism of Cu(II) interaction with the sorbed molecules [6]. A small change in donor–acceptor properties of Cu(II) ligand environment and/or a slight geometric displacement of Cu(II) ion may result in a noticeable change in hfs of the ESR signal. In situ ESR monitoring of the coordination and oxidation states of copper in Cu-ZSM-5 up to 500°C demonstrated that the Cu(II) state is stable upon treatment in vacuum or in pure He [8]. At 20–300°C, formation of adsorption complexes with NO, NO_2, and H_2O alters the coordination of Cu(II) cations. Selective reduction of the most reactive square-planar Cu(II) ions to Cu(I) by methane at 500°C was detected [9]. It was shown that at 20°C, in propene flow, the formation of an oligomeric material was accompanied by reduction of a significant part of the Cu(II) cations [10], and heating to 200–300°C led to quantitative reduction of the cupric ions. Ethanol sorption at 20°C resulted only in a coordination change of the Cu(II) by octahedral complex formation [10].

3.2. *Mo(V) cations in high-silica zeolites*

The solid-state interaction between mordenite or ZSM-5 and MoO_3 does not result in an ESR signal for Mo(V) ions after calcination in air or in vacuum [11]. Reduction of both uncalcined and pre-calcined mixtures by H_2 at 300–400°C produced identical, weak Mo(V) ESR signals. MoO_3 forms polymer fragments in vapor phase, but not cationic species. Therefore, Mo(VI) ions cannot enter into zeolitic channels, despite the high volatility of MoO_3.

After heating at 150°C, the ampule with the mixture H-ZSM-5+$MoCl_5$ in vacuum, a strong ESR signal was generated (Fig. 3). Calcination of the ampule at 350°C resulted in the sublimation of excess $MoCl_5$ (T_{melt}=268°C), but the intensity of the ESR signal did not decrease. Air was introduced at 20°C and this resulted in considerable broadening of the ESR signal (Fig. 3). However, evacuation of the sample at 20°C for 1 min led to a complete restoration of the spectrum (Fig. 3). After calcination of the mixture at 550°C for 30 min, the ESR signal retained 70% of its initial intensity. Calcination of H-mordenite (HM) with $MoCl_5$ in vacuum produced intensive Mo(V) ESR signal, but the interaction of NaM with $MoCl_5$ did not result in any noticeable formation of isolated Mo(V) ions.

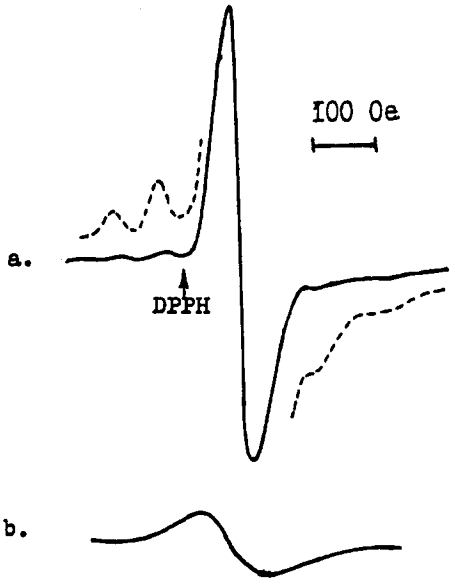

Fig. 3. ESR spectra at 20°C, of the mixture H-ZSM-5+$MoCl_5$ calcined in vacuum at 140°C: (a) in vacuum; and (b) after the introduction of air [11].

Calcination of the mixture (amorphous SiO_2–Al_2O_3+$MoCl_5$) at 150°C, as in the case of H-ZSM-5, led to a considerable Mo(V) signal. However, calcination of the sample under more severe conditions resulted in a continuous decrease in the signal intensity. The signal disappeared completely when the sample was calcined at 550°C for 30 min. So, Mo(V) in the cationic positions of zeolites was more strongly bonded than on the surface of SiO_2–Al_2O_3.

Mo(V) is not stable in H-ZSM-5 upon oxidative treatment [11]. The calcination of the Mo(V)/H-ZSM-5 sample in air at 300°C resulted in irreversible disappearance of Mo(V) ESR. The subsequent reduction by H_2 produced only a very weak Mo(V) ESR signal.

3.3. *Cr(V) stabilized by H-ZSM-5 matrix*

The thermal treatment of mixtures of high-silica H-zeolites and chromium oxides resulted in the appearance of an ESR spectra from isolated Cr(V) ions [11–13]. Calcination of the different mixtures under severe conditions produced Cr(V) ESR signals, the maximum intensities of which were determined by the number of acid sites in the zeolites.

Fig. 4 shows the ESR spectra at 20°, for the Cr/H-ZSM-5 sample, calcined in air or in vacuum. Cooling the sample to −196°C resulted in an increase in the ESR-signal intensity (g=1.98; ΔH=50 Oe). Introduction of air at 20°C gave rise to a considerable but reversible line broadening (Fig. 4c) [11]. Such a change in the ESR spectrum in O_2, caused by the dipole–dipole broadening of all components of hfs, demonstrated the accessibility of Cr(V) cations to O_2. Chemisorption of ammonia or pyridine at 20°C produced new ESR signals (superposition of two or three anisotropic signals from Cr(V) with no hfs structure) [11].

In ZSM-5, the average distance between Al atoms in the framework is large. Therefore, it is difficult to imagine a site capable of polyvalent cation coordination without additional ligands. It is suggested [11–13] that isolated complex cation species $(CrO_2)^+$, and not isolated Cr^{5+} ions, are coordinated in cation positions.

The presence of hfs in the ESR spectra from Cr(V) cations located in H-ZSM-5 (Fig. 4) is an unusual property of these samples. This splitting demonstrates the interaction between the unpaired electron of Cr(V) and the nuclear spin ($I = 5/2$) of lattice Al^{3+} ions.

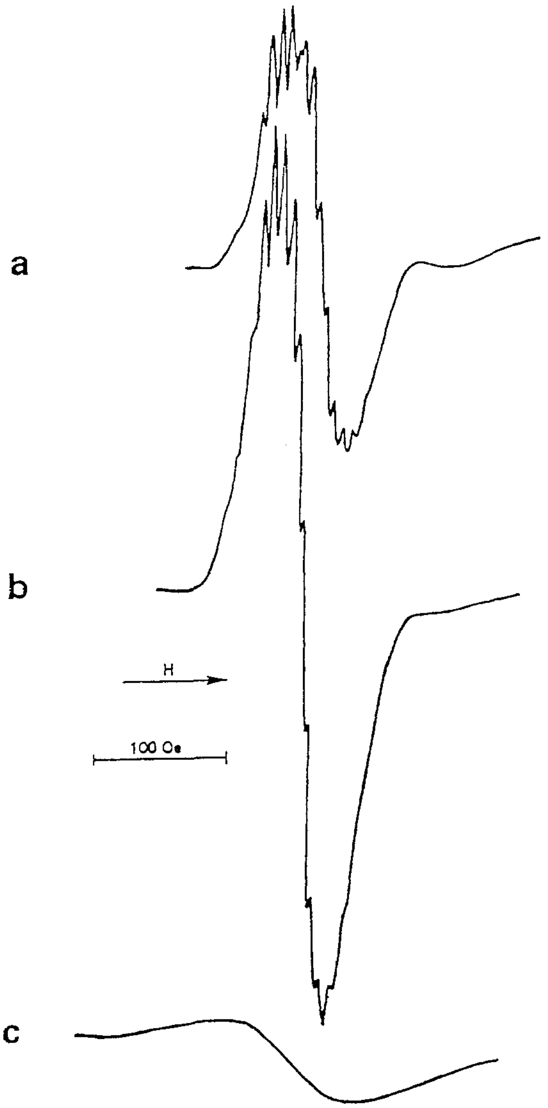

Fig. 4. ESR spectra at 20°C, of the mixture H-ZSM-5+CrO_3: (a) calcined in air at 550°C and evacuated; (b) calcined at 800°C and evacuated; and (c) after the introduction of air [11].

The spectra from Cr(V) in ZSM-5 are very well resolved in Q-band (Fig. 5) [14]. It was supposed that the Al^{3+} ion is situated in the second coordination sphere of the $(CrO_2)^+$ species.

3.4. V(IV) cations in high-silica zeolites

V(IV) is put in cationic positions via a solid-state reaction of V_2O_5 with H-ZSM-5 [11,15,16].

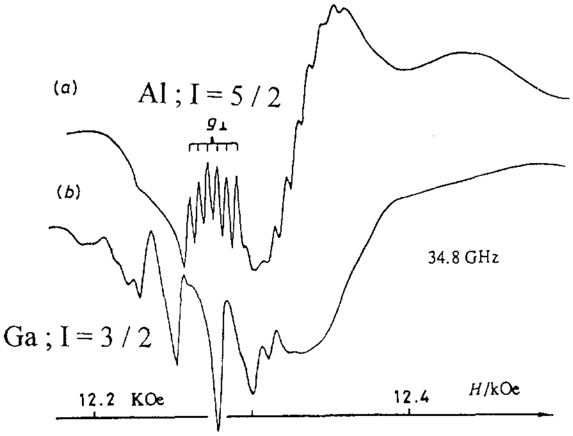

Fig. 5. ESR spectra in Q-band at 20°C, of Cr(V) cations introduced into (a) H-ZSM-5; and (b) H-[Ga]ZSM-5 [14].

Calcination of mechanical mixtures of V_2O_5 with H-ZSM-5 at 550–800°C resulted in the appearance of V(IV) ESR spectra (Fig. 6), which are typical of the isolated vanadyl species ($g_{\parallel}=1.93$; $g_{\perp}=2.00$; $A_{\parallel}=198$ Oe; $A_{\perp}=85$ Oe) [11,15]. Calcination of the mixture in air, vacuum or H_2 (60 mmHg) led to spectra, identical to that shown in Fig. 6a. The introduction of air at 20°C led to drastic but reversible line broadening. An hfs of 7 Oe was detected by recording the ESR spectra at 200°C (Fig. 6) [16]. This is an experimental evidence of electronic interaction between the vanadyl cation and the lattice Al^{3+} ion of ZSM-5 [16].

The interaction of isolated V(IV) cations in H-ZSM-5 with different molecules (ammonia, pyridine, 2,4,6-trimethylpyridine (TMPy), *p*-xylene, nitrobenzene) was also studied by ESR spectroscopy [15]. It was shown that the initial ESR spectrum is split into two spectra upon adsorption of all the molecules studied, except for TMPy. Since adsorption of sterically hindered molecules like TMPy did not affect the parameters of the ESR spectrum, it was concluded that both the V(IV) species are localized within the structure of the zeolite and not on the outer surface [15].

Adsorption of NH_3, pyridine or nitrobenzene is accompanied by a significant change in the parameters of the V(IV) ESR spectrum, due to incorporation of the strong ligands in the coordination sphere [15]. It was assumed that adsorption of ammonia or pyridine results in an increase in the covalency of the bonds due

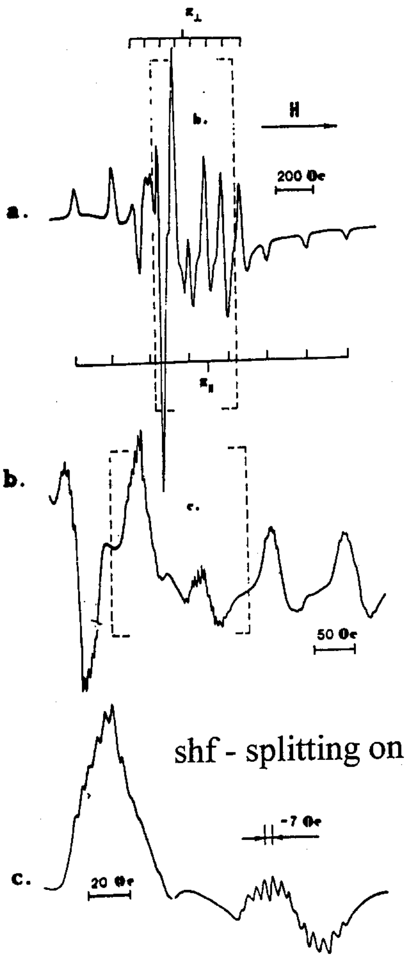

Fig. 6. ESR spectrum of isolated vanadyl cations introduced into H-ZSM-5 by a solid-state exchange with V_2O_5: (a) at 20°C; (b) and (c) are fragments of spectrum of (a) taken at 200°C [16].

to delocalization of the unpaired electron to the orbitals of the ligands. On the contrary, in adsorption of nitrobenzene, it was noted that delocalization of the electron decreases and the V–O bonds become more polar [15].

The valence state of V(IV) in the H-ZSM-5 channels is extremely stable upon redox treatment: the cation is not oxidized to V(V) even after heating in air at 800°C [11,15].

3.5. *Iron ions in H-ZSM-5*

Location, coordination and reactivity of Fe(III) cations in H-ZSM-5 were studied in comparison with those of Fe(III) lattice ions in ferrisilicate H-[Fe]ZSM-5 [17].

The solid-state interaction of H-ZSM-5 with FeO or Fe_3O_4 at temperatures up to 800°C is not accompanied by the formation of isolated Fe^{3+} ions [17]. The use of $FeCl_3$ ($T_{\mathrm{melt}}=309°C$) enabled the registration of Fe^{3+} ion migration and re-distribution at 250–300°C.

The formation of the ESR signal with $g=4.27$ is typical of isolated Fe^{3+} ions being located in a strong crystal field of low symmetry. An anomalous temperature dependence of the signal intensity was a peculiarity of the ESR signal. It was believed that cationic species with one elemental charge (FeO^+, $FeCl_2^+$) neutralizes one elemental lattice charge (AlO_4^-) [17]. Reversible broadening of Fe^{3+} ESR lines upon the introduction of oxygen, caused by the dipole–dipole interaction with O_2, demonstrated the accessibility of Fe^{3+} ions to gas-phase molecules. Interaction of coordinatively unsaturated Fe^{3+} ions with such strong ligands as ammonia or pyridine resulted in an increase in field symmetry, provoking the shift of ESR lines to smaller g-values (replacement of ESR lines with $g= 6.25$ and 5.65 by a low-temperature line with $g= 4.27$) [17].

Fe(III) cations in H-ZSM-5 could not be reduced by NH_3 at temperatures up to 300°C. The more severe treatment of the sample, at 550°C for 30 min, led to the complete disappearance of isolated Fe^{3+} ions with the formation of Fe°. Changes in Fe^{3+} ESR spectra, upon interaction of Fe-H-ZSM-5 with weak ligands such as p-xylene, confirmed the great coordinative unsaturation of the isolated Fe^{3+} cations [17].

The properties of Fe^{3+} lattice ions in ferrisilicate (tetrahedral and distorted tetrahedral environments) differed drastically from those of Fe^{3+} cations in H-ZSM-5. Molecules (e.g., NH_3) sorbed in ferrisilicate channels did not influence the symmetry of the crystal field (opposite Fe^{3+} cations), and the Fe^{3+}-lattice ions were resistant to the reductive treatment [17].

3.6. *Manganese ions in H-ZSM-5*

The valence state Mn^{2+} was identified by ESR for the part of isolated Mn cations in Mn/ZSM-5. However, these ions were unable to change the valence upon redox treatment. Therefore, it is difficult to relate the redox catalytic activity of Mn/ZSM-5 with these Mn^{2+} ions. At the same time, the H_2–O_2 titration of

Mn/ZSM-5 allows to monitor the change in the valence state for another part of Mn cations being ESR silent. It seems more likely to correlate the redox behavior of Mn/ZSM-5 catalysts with these Mn ions.

3.7. *Co-introduction of different ions into cationic positions of H-ZSM-5*

The co-introduction of (Cu^{2+} + Cr^{5+}) and (Cu^{2+} + V^{4+}) into the zeolite H-ZSM-5 by a solid-state reaction is possible under different treatment conditions [18]. Two different ions can be co-introduced in cationic positions inside zeolitic channels or one type of cation can substitute the other. The final result depends on the rate of migration, redistribution and substitution of polyvalent ions in cation sites of high-silica zeolites [18]. Different ions can be located at the same sites and migration, and re-distribution processes proceed concurrently [18].

The ESR spectrum of the calcined mixture of H-ZSM-5 and $CuCrO_4$ was the superposition of ESR signals from the isolated Cu(II) and Cr(V) ions. These ions were located in the same sites as after introduction of the individual cations from CuO or CrO_3 [2,11]. The ratio of the Cu(II) to the Cr(V) ESR signal intensities was estimated to be of the range 2–3 [18].

Cr(V) ions in the cation positions of the H-ZSM-5 can be exchanged for Cu(II) ions upon oxidative calcination of the binary mixture. The Cu^{2+}/Cr^{5+} ratio reached 20–30. Reduction of the sample containing co-introduced Cu(II) and Cr(V) cations by H_2 resulted in a rapid disappearance of ESR signals from both isolated Cu^{2+} and Cr^{5+} cations [18].

An examination of the interaction of H-ZSM-5 with V_2O_5 and CuO was conducted under different conditions [18]. In was shown that, in an oxidative atmosphere, Cu(II) ion was bound more strongly in the cationic position than the V(IV) ion, and vanadium was displaced from the zeolite channels to the outer surface of crystals and oxidized to V(V). Reduction by H_2 at 400°C resulted in a sharp decrease in Cu(II) cation concentration, but no subsequent increase in V(IV) ion concentration. This temperature was too low to promote the migration of vanadyl ions from the outer surface of the crystals. However, the rise in temperature to 800°C in H_2 led to a quick re-migration of V(IV) ions into vacant cationic sites and the intensity of the V^{4+} ESR signal returned to the initial value. A new oxidative treatment of the reduced binary sample resulted in the repeated replacement of almost all V(IV) cations by the Cu(II) ions formed.

The effect of cation substitution was more pronounced in the Fe^{3+}/H-ZSM-5+CuO system [17]. At least 99% of isolated Fe^{3+} cations were replaced by Cu(II) cations as a result of high-temperature interaction between Fe^{3+}-containing H-ZSM-5 and copper oxide. Also, the concentration and coordination of Cu(II) ions, introduced into the sample by a solid-state exchange, coincided completely with those of Cu(II) cations in Cu/H-ZSM-5 [3].

However, no replacement of Cu^{2+} for Co^{3+} was detected upon impregnation of Cu-ZSM-5 with $Co(NO_3)_3$ solution and subsequent calcination up to 600°C [19].

The solid-state interaction does not permit the exchange of Na^+ cations in H-ZSM-5 for polyvalent cations, i.e., the strength of linkage for Na^+ ion exceeds noticeably the bonding strength for all transition-metal ions studied. Formally, the strength of retention of different ions in cationic positions of H-ZSM-5 decreases in the order: $Na^+ \gg Cu^{2+} > Cr^{5+} > V^{4+}, Co^{3+}, Fe^{3+}$.

4. Cations of transition metals as active catalytic sites in H-ZSM-5

The ability of the H-ZSM-5 matrix to stabilize transition-metal ions, as isolated cationic species being located in unusually low-coordination environments (Cu^{2+}, Fe^{3+}) and non-typical valence states (Cr^{5+}, V^{4+}), is demonstrated above. Such coordinatively unsaturated sites are very reactive toward a variety of ligands. Therefore, such systems are interesting from the catalytic point of view. Moreover, thermal treatment of the samples as well as the introduction of different anionic ligands (F^-, SO_4^{2-}, PO_4^{3-}) permits the local topography of the isolated cationic sites to be changed. So, the comparative catalytic testing of such systems enables one to elucidate the influence of local crystal-field symmetry on the intrinsic catalytic properties of isolated transition-metal ions.

In spite of the fact that the number of active sites in high-silica zeolites is small (1–1.5 wt% of transition-metal oxide may only be located in zeolitic matrix in catalytically active form), there are some examples of very high intrinsic redox activity in H-ZSM-5. Some recent works show that modification of pentasils by transition-metal cations permits to prepare active and stable catalysts for both total oxidation of alkanes and NO decomposition.

4.1. *Cu/H-ZSM-5 zeolite as catalyst for both NO decomposition and NO reduction with hydrocarbons*

Catalytic decomposition of nitric oxide was studied on a number of zeolites containing transition-metal cations, but of these, only the Cu^{2+} forms showed appreciable activity. The conversion of NO showed an S-shaped dependence on the exchange level. It was assumed that at least two kinds of sites exist in the ZSM-5. Pure H-form of ZSM-5 was inactive in stoichiometric NO decomposition.

SO_3 deactivates Cu/H-ZSM-5 for NO decomposition due to the formation of $CuSO_4$-type species. Nitric-oxide reduction with hydrocarbons was a complex process which takes place on H-forms of zeolites. However, the introduction of different cations into the zeolite noticeably changed the activity of catalysts. Cu/H-ZSM-5 was the most active for the selective reduction of NO by ethene in the presence of oxygen at temperatures as low as 437–573 K. No detailed study of the reaction mechanism or active-site structure was realized, but the assistance of Cu^+ ion in the process was assumed.

In situ ESR monitoring of Cu/H-ZSM-5 at 300–500°C in flowing mixtures ($NO+C_3H_6+O_2$) demonstrated that the equilibrium oxidation state of copper depended on both the temperature and the composition of the gas mixture [10]. At 500°C, in an excess of oxygen, the condition prevailing during SCR, virtually all of the copper remains in the Cu(II) state. The reoxidation of any reduced site by O_2 (or NO_2) is very fast. Only at lower temperatures and/or close to stoichiometry does the equilibrium $Cu^{2+} <-> Cu^+$ begin to shift to the right [10].

The difference between the stability of the transition-metal sites in Cr-ZSM-5 and Cu-ZSM-5, under identical conditions, is shown in [13]. In conditions typical during SCR, even with a large excess of oxygen, the relative extent of reduction of the Cr(V) cations in Cr-ZSM-5 is much higher than that of Cu(II) cations in Cu-ZSM-5 [13].

4.2. *Complete oxidation of alkanes*

Catalytic oxidation of CH_4 traces with O_2 is enhanced using cation-containing H-ZSM-5 zeolites instead of H-ZSM-5 [20–24]. The system permits to compare intrinsic activities of different ions (or of the same ions in different local environments).

4.2.1. *Cr/H-ZSM-5*

Supported chromia catalysts (Cr/SiO_2; Cr/SiO_2–Al_2O_3) are well-known active catalysts for complete oxidation. A comparative study of Cr/H-ZSM-5 with known physical properties is of interest. Fig. 7 shows the activity of Cr/H-ZSM-5 in CH_4 burn-up at 500°C [20–22]. Catalytic activity of the Cr/H-ZSM-5 system increased linearly with the rise of chromium content up to 1.5 wt%, showing considerable site homogeneity. The activity of the catalyst reached a maximum when the number of isolated Cr(V) cations, capable of changing valence state upon redox treatment, reached a maximum. So, the excess of chromia (α-Cr_2O_3 phase on the outer surface of zeolitic crystals) did not contribute to the catalytic activity of the samples. At the same time, it was shown that the specific activity of Cr(V) cation in H-ZSM-5 is much higher (by a factor of 30) than that of Cr(V) ion stabilized on the surface of amorphous supports [20–22]. We

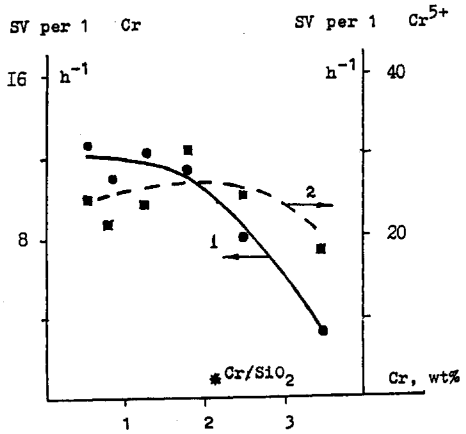

Fig. 7. Space velocity (SV) (99% methane conversion, 500°C) for different Cr/H-ZSM-5 samples: (1) total; and (2) per gram of Cr(V) [21].

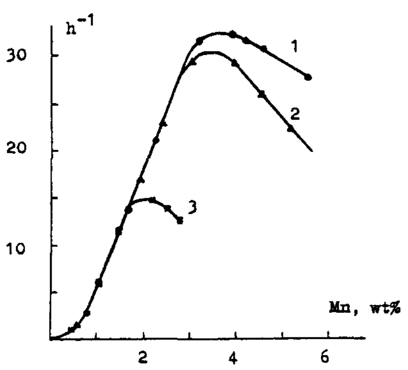

Fig. 8. Space velocity (SV) (99% methane conversion, 500°C) for Mn/H-ZSM-5 samples with different Al content in zeolites with: (1) Si/Al=16; (2) Si/Al=20; and (3) SiAl=40 [23].

assume that stabilization of the isolated Cr(V) ions in coordinatively unsaturated environment inside H-ZSM-5 is a reason of such unusually high intrinsic catalytic activity.

4.2.2. *Mn/H-ZSM-5*

Complete oxidation of CH_4 over Mn/H-ZSM-5 proceeds with very high activity and stability [22,23]. Fig. 8 shows the dependence of catalytic activity upon the Mn content in H-ZSM-5 samples, with different SiO_2/Al_2O_3 ratios [23]. It was concluded that (1) the maximum number of catalytic sites (i.e., isolated Mn cations) depends linearly on the concentration of vacant acid sites in H-ZSM-5; and (2) intrinsic activity per Mn ion in Mn/H-ZSM-5 exceeds that in Mn/SiO_2 by a factor of 10 [23].

4.2.3. *Cu/H-ZSM-5*

Catalytic oxidation of CH_4 with O_2 using Cu^{2+}-containing H-ZSM-5 was studied in detail [24]. Fig. 9 shows the activity for different Cu/H-ZSM-5 samples. Catalytic activity of Cu/H-ZSM-5 increased within the first 5–10 min on-stream and then reached a steady state. No reduction in the effectiveness of the catalysts was found at 500°C after 10 h of continuous use. The calcination of the sample in air at 550°C for 15 h did not result in any decrease in the catalytic activity [24].

It is clearly seen from Fig. 9 that stabilization of Cu(II) ions in H-ZSM-5 results in the formation of active sites. At the same time, an increase in the activity per gram of Cu (Fig. 9, curve 2) demonstrates the inhomogeneity of catalytic sites. By comparison of catalytic data with the results, obtained from the study of Cu^{2+} location and coordination, it was concluded that the high catalytic activity is determined only by the formation of the most coordinatively unsaturated square-planar Cu(II) ions [24]. A linear correlation between the amount of square-planar Cu(II) and the activity of the Cu/H-ZSM-5 sample demonstrated the decisive role of these [24].

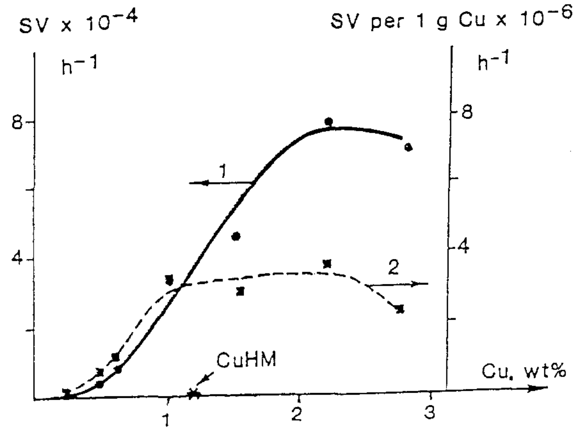

Fig. 9. Space velocity (SV) (99% methane conversion, 500°C) for different Cu/H-ZSM-5 samples: (1) total; and (2) per gram of Cu [24].

When the number of isolated Cu(II) cations in the zeolite reached a maximum (at 1.5–2.0 wt% Cu), the activity of the catalyst also reached a limit (Fig. 9, curve 1). The excess CuO on the outer surface of the zeolite did not contribute noticeably to Cu/H-ZSM-5 catalytic activity in CH_4 oxidation [24].

The calcination of the Cu/H-ZSM-5 sample at 800°C for 1–2 h did not noticeably reduce the number of isolated Cu(II) ions accessible to reagents, but a considerable change in the Cu(II) ligand environment occurred. The most unsaturated square-planar Cu(II) coordination disappeared completely as a result of high-temperature treatment, and a 1000-fold drop in catalytic activity of the samples accompanied the change in the local topography of isolated Cu(II) in catalytic sites [24]. The samples Cu/HM and CuO/SiO_2 (which did not contain square-planar Cu(II)) also showed a much lower specific activity than Cu/H-ZSM-5.

The relation between catalytic activity and Cu^{2+} site local topography has already been studied (see

Ref. [25]). The same samples Cu/H-ZSM-5 and Cu/HM were tested in catalytic ethane oxidation, but catalyst activities were measured at low alkane conversion. The samples did not differ noticeably in the total number of accessible active Cu(II) sites diluted in an inert support, and the specific activity per cupric ion was compared in each case. It was shown that a 1000-fold change in the specific activity of the isolated Cu^{2+} site may occur as a result of local topography transformation [25]. Activity of the sample Cu/H-ZSM-5 (500°C, which contained the most coordinatively unsaturated square-planar Cu(II) ions) exceeded activities of the samples containing five-coordinated Cu^{2+} ions by a factor ranging 30–100. Subsequent transformation of Cu(II) environment to the most symmetrical octahedral form resulted in a further activity fall by a factor of 30. Suppression of complete oxidation was accompanied by a selectivity change: an activity in high-temperature partial oxidation became measurable for the samples with more symmetrical Cu environments [26].

The change of the topology of the most active coordinatively unsaturated Cu(II) cations, upon introduction of sulfate anions in Cu-ZSM-5, results in the same effect of drastic decrease in the intrinsic activity of the active redox site [4].

The decisive role of the most reactive, square-planar isolated cupric ions, was also confirmed in Ref. [27], where the reactivity loss upon high-temperature calcination and steam-ageing of Cu-ZSM-5 was studied.

Kinetics of catalytic methane oxidation on Cu-ZSM-5 was studied in detail recently [28]. It was shown that, in the kinetic region, the reaction rate depended linearly on methane concentration. To evaluate the possible influence of the reaction products, their content in the reaction mixture was varied over a wide range, and no influence of either O_2 or CO_2 was detected. Water vapors reduce the reaction rate noticeably, but this influence is completely reversible. The results obtained are described by a rather simple kinetic equation, and the reaction scheme is proposed [28].

4.2.4. V/H-ZSM-5

The system V/H-ZSM-5 with isolated V(IV) cations was completely inactive in CH_4 burn-up [22], due to the stability of the V(IV) valence state [11,15]. Introduction of V into H-ZSM-5 zeolite does not permit to prepare active catalysts for complete alkane oxidation.

4.3. Thermal stability of H-ZSM-5 containing transition-metal cations as catalytic sites

The mechanism of Cu/H-ZSM-5 deactivation upon the high-temperature treatment is not fully understood. In a recent work [27], an attempt was made to monitor the physical changes in the Cu-ZSM-5 structure accompanying the high-temperature dry or wet deactivation of the catalyst. It was demonstrated that steam-ageing (630°C) or dry calcination (850°C) induced a change in Cu(II) coordination without noticeable agglomeration or encapsulation of the isolated ions. At the same time, the reactivity and ability of the Cu(II) sites to adsorb different molecules was substantially affected. Therefore, the loss of catalytic activity was associated with irreversible changes in the local topography of the Cu(II) sites [27].

A stabilizing effect was noted for bicationic Cu-ZSM-5 samples modified by a relatively large amount of multivalent rare-earth ions, namely La or Ce [29]. These modifiers markedly attenuated the spatial rearrangement of the Cu(II) ions during high-temperature calcination. The loss of catalytic activity in ethane oxidation of either Cu-ZSM-5 or Cu/La-ZSM-5 after high-temperature treatment correlates well with the loss of the isolated Cu(II) sites located in the most reactive square-planar coordination, as the comparison of Fig. 10 with Fig. 11 illustrates.

5. Concluding remarks

1. The pentasil-type matrix is capable of stabilizing isolated cations in both non-typical valence states and unusually low-coordination environments (i.e., in local crystal fields of low symmetry). Such coordinatively unsaturated transition-metal ions have very high reactivity. The presence of different anionic ligands results in the change in the local topography of the cationic site. Therefore, an atomic-scale engineering of catalytic functions of isolated active sites in confined environments of zeolitic channels becomes possible.
2. Pentasil-based catalysts with discrete, isolated redox sites permit a correct study of structure–

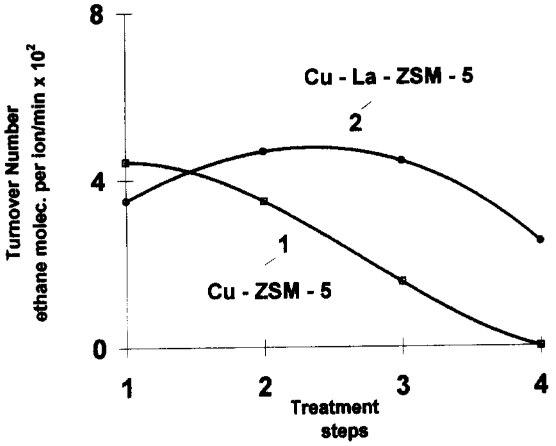

Fig. 10. Change in the relative concentration of the square-planar Cu(II) ions after stepwise calcination of the samples: (1) 1.27% Cu-ZSM-5; and (2)1.06% Cu/5.4% La-ZSM-5 [29].

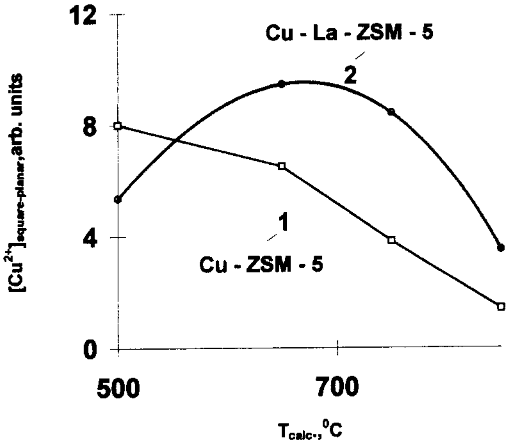

Fig. 11. Specific activity in ethane oxidation at 330°C, after stepwise calcination of the samples: (1) 1.27% Cu-ZSM-5; and (2) 1.06% Cu/5.4% La-ZSM-5 [29].

activity relationship for isolated active sites of known local topography.

3. In spite of the fact that the concentration of active sites in high-silica zeolites cannot be high, there are some examples of very high specific redox activity of 'biomimetic' cationic sites stabilized by H-ZSM-5 matrix. Some recent works show that modification of pentasils by transition-metal cations permits the preparation of promising catalysts both for complete oxidation of alkanes and NO_x decomposition.

References

[1] A.V. Kucherov and A.A. Slinkin, J. Mol. Catal., 90 (1994) 323.
[2] A.V. Kucherov and A.A. Slinkin, Zeolites, 6 (1986) 175.
[3] A.V. Kucherov, A.A. Slinkin, D.A. Kondratyev, T.N. Bondarenko, A.M. Rubinstein and Kh.M. Minachev, Zeolites, 5 (1985) 320.
[4] A.V. Kucherov, S.S. Goryaschenko, T.N. Kucherova, K.I. Slovetskaya and A.A. Slinkin, Kinetika I Kataliz, 34 (1993) 1089.
[5] L. Zhenyi, Z. Wangjin and Y. Quin, Proceedings of the 7th International Zeolite Conference, Tokyo, 1986, Kodansha-Elsevier, Tokio–Amsterdam, 1986, p. 1091.
[6] A.A. Slinkin, A.V. Kucherov, N.D. Chuvylkin, V.A. Korsunov, A.L. Kliachko and S.B. Nikishenko, J. Chem. Soc., Faraday Trans. 1, 85 (1989) 3233.
[7] A.V. Kucherov and A.A. Slinkin, J. Phys. Chem., 93 (1989) 864.
[8] A.V. Kucherov, J.L. Gerlock, H.-W. Jen and M. Shelef, Zeolites, 15 (1995) 9.
[9] A.V. Kucherov, J.L. Gerlock, H.-W. Jen and M. Shelef, Zeolites, 15 (1995) 15.
[10] A.V. Kucherov, J.L. Gerlock, H.-W. Jen and M. Shelef, J. Catal., 152 (1995) 63.
[11] A.V. Kucherov and A.A. Slinkin, Zeolites, 7 (1987) 38.
[12] A.A. Slinkin, A.V. Kucherov, S.S. Goryashenko, E.G. Aleshin and K.I. Slovetskaya, Zeolites, 10 (1990) 111.
[13] A.V. Kucherov, C.P. Hubbard and M. Shelef, Catal. Lett., 33 (1995) 91.
[14] A.V. Kucherov, A.A. Slinkin, H.K. Beyer and G. Borbely, J. Chem. Soc., Faraday Trans 1, 85 (1989) 2737.
[15] A.A. Slinkin, A.V. Kucherov and S.B. Nikishenko, Kinetika I Kataliz, 31 (1990) 692.
[16] A.V. Kucherov and A.A. Slinkin, Zeolites, 7 (1987) 583.
[17] A.V. Kucherov and A.A. Slinkin, Zeolites, 8 (1988) 110.
[18] A.V. Kucherov and A.A. Slinkin, Zeolites, 7 (1987) 43.
[19] A.V. Kucherov, T.N. Kucherova and A.A. Slinkin, Kinetika I Kataliz, 36 (1995) 731..
[20] A.A. Slinkin, A.V. Kucherov, S.S. Goryashenko and K.I. Slovetskaya, Proceedings of All-Union Conference, Use of zeolites in catalysis, Moscow, Nauka, 1989, p. 191.
[21] A.A. Slinkin, A.V. Kucherov, S.S. Goryaschenko, E.G. Aleshin and K.I. Slovetskaya, Proceedings of the 8th Soviet–French Seminar on Catalysis, Novosibirsk, 1990, p. 153.
[22] A.A. Slinkin, A.V. Kucherov, S.S. Goryaschenko, E.G. Aleshin and K.I. Slovetskaya, Proceedings of the 9th Soviet–Japanese Seminar on Catalysis, Novosibirsk, 1990, p. 224.
[23] S.S. Goriashenko, K.I. Slovetskaya, M.A. Alimov and A.A. Slinkin, Kinetika I Kataliz, 33 (1992) 350.

[24] A.V. Kucherov, A.A. Slinkin, S.S. Goryashenko and K.I. Slovetskaya, J. Catal., 118 (1989) 459.
[25] S.S. Goriashenko, K.I. Slovetskaya, A.V. Kucherov and A.A. Slinkin, Kinetika I Kataliz, 30 (1989) 249.
[26] A.V. Kucherov, T.N. Kucherova and A.A. Slinkin, Catal. Lett., 10 (1991) 289.
[27] A.V. Kucherov, C.P. Hubbard and M. Shelef, J. Catal., 157 (1995) 603.
[28] N.V. Nekrasov, A.A. Slinkin, G.O. Bragina, A.V. Kucherov, E.A. Katsman and S.L. Kiperman, Kinetika I Kataliz, 1997, in press.
[29] A.V. Kucherov, C.P. Hubbard, T.N. Kucherova and M. Shelef, Appl. Catal. B: Environmental, 7 (1996) 285.